Journal of Materials Chemistry B

Versatile Multicolor Nanodiamond Probes for Intracellular Imaging and Targeted Labeling

Journal:	*Journal of Materials Chemistry B*
Manuscript ID	TB-ART-02-2018-000508.R1
Article Type:	Paper
Date Submitted by the Author:	27-Mar-2018
Complete List of Authors:	Bray, Kerem; University of Technology Sydney, School of Mathematical and Physical Sciences Cheung, Leonard; University of Technology Sydney, School of Mathematical and Physical Sciences Hossain, Khondker ; University of Technology, Sydney, School of Life Sciences; University of Technology Sydeny, ARC Research Hub for Integrated Device for End-user Analysis at Low-levels (IDEAL) Aharonovich, Igor; University of Technology, Sydney, School of Mathematical and Physical Sciences; University of Technology Sydeny, Institute of Biomedical Materials and Devices (IBMD); University of Technology Sydeny, ARC Research Hub for Integrated Device for End-user Analysis at Low-levels (IDEAL) Valenzuela, Stella; University of Technology Sydney, School of Life Sciences; University of Technology Sydeny, ARC Research Hub for Integrated Device for End-user Analysis at Low-levels (IDEAL) Shimoni, Olga; University of Technology Sydney, School of Mathematical and Physical Sciences; University of Technology, Sydney, Institute of Biomedical Materials and Devices (IBMD); University of Technology Sydeny, ARC Research Hub for Integrated Device for End-user Analysis at Low-levels (IDEAL)

Versatile Multicolor Nanodiamond Probes for Intracellular Imaging and Targeted Labeling

Kerem Bray[§], Leonard Cheung[§], Khondker Rufaka Hossain[†‡], Igor Aharonovich[§‡], Stella M. Valenzuela[†‡], and Olga Shimoni[§‡]*

[§]Institute of Biomedical Materials and Devices (IBMD), Faculty of Science, University of Technology Sydney, Ultimo, NSW, 2007, Australia

[†]School of Life Sciences, Faculty of Science, University of Technology Sydney, Ultimo, NSW, 2007, Australia

[‡]ARC Research Hub for Integrated Device for End-user Analysis at Low-levels (IDEAL), Faculty of Science, University of Technology Sydney, Ultimo, NSW, 2007, Australia

Corresponding author: olga.shimoni@uts.edu.au

KEYWORDS

nanodiamonds, bio-imaging, fluorescent probes, silicon-vacancy centers

ABSTRACT

We report on a sizable production of fluorescent nanodiamonds (FNDs) containing a near infrared (NIR) color center – namely the silicon vacancy (SiV) defect, and their first demonstration inside cells for bio-imaging. We further demonstrate a concept of multi-color bio-imaging using FNDs to investigate intercellular processes using two types of FNDs. Due to their specific spectral properties, SiV FNDs can be distinguished from common nitrogen-vacancy (NV) FNDs and showed a distinct initial spreading throughout the cell interior. The reported results are the first demonstration of multi-color labeling with FNDs that especially interesting for in vivo bio-imaging due to stable fluorescence of FNDs.

TEXT

Targeted sub-cellular imaging is crucially important for understanding biological processes and developing new drugs. To this extent, fluorescent probes are sought after for a range of potential applications, from mapping cellular environments, measuring cell temperatures and amino acids concentrations to monitoring drug localization within the body.[1-5] Despite numerous advantages, majority of fluorescent probes, such as quantum dots or fluorescent proteins, exhibits undesirable properties, including blinking, photo-bleaching and/or toxicity, limiting their use for biological imaging.[6, 7]

Fluorescent nanodiamond[8,9] particles (FNDs) are a promising material for bio-sensing and bio-imaging due to their ability to host a variety of bright, photostable color centers originated from atomic defects in the carbon lattice.[10,11] Furthermore, FNDs possess inherent biocompatibility and high surface tunability.[12-14] To date, there is abundance of research on the application of FNDs containing nitrogen-vacancy (NV) defects for bio-imaging and drug delivery.[15-22] However, NV FNDs have excitation and emission in visible range that can contribute to tissue absorption and auto-fluorescence. Therefore, FNDs with emission at the near infra-red (NIR) spectral range are particularly advantageous to achieve a better signal to noise ratio imaging for long term cellular imaging.[23] In addition, excitation of NIR emitters can be achieved using a longer wavelength, therefore minimizing tissue light absorption. Finally, use of NIR luminescent probes is valuable in bio-imaging as it presents a greater tissue penetration depth comparing to visible range fluorophores.[23]

One defect that meets these criteria is the silicon vacancy (SiV) color center in diamond that has narrowband emission at 738 nm. Despite clear advantages of SiV ND properties, reliable

fabrication and application of SiV FNDs for sustained biological applications remains a pressing issue and challenge.[24]

In our work, we report on a scalable approach to produce FNDs hosting the SiV emitters, confirm that the fabricated nanoparticles hold NIR fluorescent properties and with sizes compatible for bio-imaging. The SiV color center is ideal as it can fluoresce in the near infra-red region, which allows us to excite the sample at higher wavelengths which reduces cell autofluorescence. We further demonstrate the concept of utilization of FNDs as multi-color staining for intercellular immunofluorescence. In fact, for the first time we show simultaneous labeling of cell interior using two different types of FNDs, such as containing SiV and NV defects. Simultaneous labelling provides additional possibilities in a cell labeling bio-imaging. Similar to conventional fluorescent dyes, nanodiamonds offer labeling capability of cell sub-structures. For instance, owing to versatility of nanodiamond surface chemistry, two non-overlapping color FNDs can simultaneously and individually label cell surface and lysosomes. Besides this, the surface functionalization of FNDs provides additional potential functionalities that can be utilized for various applications, such as attachment of broader range of drug and sensing agents, simply superseding the simple functionality of fluorescent dyes. Diamond surface can be easily modified to attach targeting biomolecules using standard chemical procedures, such as carbodiimide chemistry[25], to achieve a specific labeling. Additionally, we can effectively resolve two types of FNDs within cells by their specific spectral properties, where we find that SiV FNDs dispersed throughout the cell interior and NV FNDs localized in a perinuclear area of cell. Finally, we show long term imaging of FNDs up to 5 hours, where timed uptake of FNDs show cell induced mechanism of FNDs aggregation. Our results are the first

demonstration of multi-color labeling with FNDs that particularly relevant for in vivo bio-imaging and drug delivery applications.

The SiV containing FNDs have been produced via bead-assisted sonication disintegration (BASD) process,[26,27] where chemical vapor deposition (CVD) grown diamond polycrystalline thin films were crushed into nanoparticles. The flow of the fabrication process is shown in **Figure 1**. Diamond nanocrystalline film is grown on a silicon substrate, where during the diamond growth (plasma of mixture of hydrogen and methane gases) silicon atoms from substrate are incorporated in a diamond lattice. The incorporation of silicon atoms leads to creation of SiV defect in the diamond nanocrystalline film. The diamond films are further processed to yield diamond nanocrystalline particles. The process of fabrication of FNDs can be upscaled depending on the capacity of CVD reactor.

Raman spectroscopy has unambiguously showed the characteristic diamond peak at 1332 cm^{-1} (**Figure S1** b) in the produced SiV FNDs. To prove that the diamond particles host bright SiV color centers, SiV FNDs were characterized using a home built scanning confocal microscope using a 532 nm excitation source through a high numerical aperture (NA = 0.9) objective at room temperature (**Figure S1** d). SiV FNDs spectra show a distinctive sharp peak centered in 737 nm.

The FNDs containing NV color centers (FND Biotech Ltd, Taiwan) with a particle size of ~35 nm, were pre-characterized for optical properties using the same home build confocal system. **Figure 2**a shows the photoluminescence spectra, where we observed the characteristic zero phonon line (ZPL) at 737 nm and 640 nm for the SiV (red) and NV (blue) color centers, respectively. NV FNDs produce a broad red fluorescence ranging from 640 to 730 nm, while SiV FNDs show a sharp narrow peak ranging between 735 to 760 nm. Two types of FNDs can

be precisely distinguished using their spectral characteristics. The nanodiamonds are stable at room temperature[10,28] and further characterization using transmission electron microscopy is shown in **Figure S2.**

The size and zeta potential of both types of FNDs were characterized by Zetasizer Nano ZS (Malvern Instruments Ltd) to test its suitability for bio-applications (**Figure 2**b). The measurements of size show the FNDs to be 141.1±49.4 nm and 44.8±13.7 nm in diameter with a zeta potential of -17.4±3.7 mV and -45.4±21.2 mV for the diamonds containing SiV and NV color centers, respectively (**Table S1**). The origin of negatively charged zeta potential on NV and SiV FNDs is due to oxidation treatments that FNDs were subjected during the purification processes that produced oxygen-containing groups, such as carboxylic, hydroxyl or ester groups. The results confirm that the ND samples are relatively small, stable and dispersed in aqueous solution that is suitable for bio-applications. By upscaling the fabrication of FNDs hosting varying color centers and modifying the surface, FNDs may target various beneficial or harmful cells to investigate cellular processes in living organisms.

The goal of our work is to demonstrate multiple, distinct cellular targeting via conjugation of FNDs with targeting species. To this end, we utilize the convenience of carbon surface functionality to attach biomolecules to achieve biologically active nanoprobes. Specifically, FNDs containing NV centers were conjugated with trans-activating transcriptional activator (TAT, China Peptides Ltd, 1mg/mL) peptides using carbodiimide chemistry. TAT peptide is a small basic cell penetrating peptide (CPP) and is known for successful cell membrane penetrating functionality that is effective at delivering materials of varying sizes from small particles to proteins into primary and other cells.[29-31] The successful conjugation was monitored by a surface charge change from -45.4±21.2 mV to +32.8±5.6 mV due to multiple positively

charged lysine residues on the peptide chain. On the other hand, the non-conjugated SiV containing FNDs can be used to target endosomes.

Cell viability studies demonstrated that at the tested concentrations of FNDs, two different types of cells, Chinese Hamster Ovarian cell line (CHO K1) and U937 macrophages, show good viability after 4h and even after 24h (**Figure S3**). Tested concentrations of FNDs were below 100 μg/mL in accordance to multiple studies on similar nanoparticles.[32-34] A student t-test conclusively shows that fluctuations in cell viability are not statistically significant, meaning that the FNDs are non-toxic to the cells at the tested concentrations.

Biological imaging studies were performed using two types of cells that were individually incubated with FNDs solutions in cell media (see Supporting Information for more details). Typically, 50 μg/mL of FNDs (SiV or NV-TAT or 50:50 ratio of SiV with NV-TAT) were mixed with cell media, added drop wise to the growing cell culture and incubated for 3 hours. The cells were subsequently fixed with a 4% paraformaldehyde/PBS solution, stained with a nucleus stain, NucBlue (Life Technologies, Australia), and subsequently imaged using an A1 Nikon confocal scanning laser microscope at room temperature equipped with 405 nm, 488 nm and 561 nm excitation laser sources.

The two types of FNDs – namely the ones containing the NV centers and the ones containing the SiV centers, can be individually distinguished based on their spectral differences (**Figure S4**). Explicitly, NV FNDs produce emission in the 620-720 nm region as a distinguished broad peak (**Figure S4** b,c), while SiV FNDs generate a sharp peak in the region of 720-750 nm (**Figure S4** d). The fluorescence of FNDs is stable with no photobleaching effect, it can help in understanding complex biological processes happening inside cells over the time. Furthermore,

excitation with 561 nm laser allowed us to avoid a large amount of auto-fluorescence that usually generated by use of blue laser, such as 475 nm, for excitation of NV defects in diamond.

Figure 3 (a-d) shows the efficient uptake of FNDs hosting SiV color centers (50 μg/mL) from cell media into the cells after 3 hours of incubation. Confocal microscopy revealed that the internalization is relatively spontaneous, without additional chemical or mechanical force. Previous studies by others have demonstrated that internalization of FNDs occurs through endocytosis.[33,35] It can be seen that SiV FNDs appear to spread over the entire cell interior (**Figure 3** b,d), while NV FNDs with TAT peptide are localized to discrete areas (**Figure 3** e-h) at the same time point. As both types of FNDs have been well dispersed in a cell media prior to cellular uptake, it is most likely that the nanoparticles processed differently once inside cells. FNDs hosting NV color centers would be internalized via a different non-receptor mediated process as their surface is conjugated with the TAT peptide (**Figure 3** e-h) with highly positive charge leading to faster cellular response.

The NV FND-TAT particles in combination with non-modified SiV containing FNDs (50:50 ratio) incubated together with cells allow the dual tagging of CHO-K1 cells. We provide a detailed spectral analysis of nanoparticles inside cell (**Figure S5**), where spectral emission of each fluorescent region clearly identifies the type of FNDs. Consequently, **Figure 3** (i-l) show successful dual tagging of the CHO-K1 cells containing FNDs hosting either SiV or NV color centers. Each red spot in **Figure 3** was confirmed by spectral distinction to be FNDs containing either NV or SiV color centers (only few labeled for clarity). It can be clearly seen that the NV FNDs (blue circles) preferentially accumulate at the periphery of the nucleus, while the SiV emitters (green circles) are dispersed throughout the cell cytoplasm. On contrary, **Figure 3** (m-p) shows the control, non-treated CHO-K1 cells with no fluorescence.

To further extend the work, we also show that all the types of FNDs internalize efficiently into macrophages. **Figure 4** unambiguously shows the positions of the FNDs in the representative 3D reconstructed confocal z-stack, where individual images from different channels (blue, red and wide field) taken at varying heights are spliced together to create a 3D rendering of the sample. The obtained z-stack images confirm that the FNDs are being internalized by the cells, with NV FNDs-TAT accumulate in perinuclear area, but are not entering the nucleus of the cells. Again, SiV FNDs were observed individually spread in the cytoplasmic area of cells. More 3D reconstructed images can be found in the supporting information (**Figure S6** (CHO K1) and **Figure S7** (U937 macrophages). This shows potential that the two types of FND particles can be used as dual tags in a cellular environment.

The efficiency of uptake for the FNDs particles into the CHO-K1 cells was also studied. A 50 μL solution of FNDs containing either NV or SiV color centers was introduced into the cultured CHO-K1 cells as described previously, then subsequently fixed and stained after 5, 30, 60, 180 and 300 minutes of incubation at 37°C. **Figure 5** (a-e) shows confocal images of the cells after the various times of incubation. After 5 minutes of incubation, **Figure 5**a show a small number of FNDs have been successfully uptaken by the CHO-K1 cells and dispersed close to a cellular membrane. **Figure 5** (a-e) shows that the FNDs particles are efficiently uptaken into the cells after 2 hours (between 1 and 3 hours of incubation) in accordance with other reports.[33, 36] Previous studies demonstrated that FNDs are internalized via endocytic pathways, where the particles are engulfed, then suspended within small vesicles (endosomes). It has been shown for other cell lines that the FNDs are usually trapped in endosomes for an hour prior to translocation to the cytoplasm.[35,37] This did not appear to be the case here, as the FNDs appear to accumulate in subcellular vesicles. As the time increases from 5 to 300 minutes, we further observe that the

FND particles are agglomerating inside the cell. This timed subcellular processing has been recently described for other type of inorganic nanoparticles (gold nanoparticles).[38] Cells initially uptake individual nanoparticles engulfed in earlier endosomes, followed by vesicular clustering and maturization, nanoparticles accumulate in late endosomes and further led into lysosomes. Such subcellular processing is indicative for intracellular trafficking of external material. In our case, we detect that after 300 minutes, the FNDs form large aggregates in perinuclear area, the same area where lysosomes are located inside the CHO-K1 cells. It is a known phenomenon that some types of nanoparticles induce a process of autophagy,[39-41] in which cells can induce autophagy pathways to eliminate these extraneous particles. Further studies are required to confirm the fate of these particles. Despite it, controlled agglomeration of nanoparticles can lead to novel applications in drug delivery applications inclusive of controlled and sustained release of a drug into biological systems.[42]

To better determine the localization of the FNDs within the cells, co-localization staining studies were undertaken using antibodies against LAMP1 (Lysosomal-associated membrane protein). LAMP1 primarily stains the late endosomes or lysosomes (**Figure 5**f). There is no visible co-localization of fluorescence in **Figure 5**f. To ambiguously confirm the co-localization of fluorescence, we perform co-localization tests (**Table 1,** Pearson's coefficient, Manders Coefficient, Costes P-value and Li's intensity correction quotient (ICQ) explained in Supporting Information).

The Pearson's R value for the LAMP1 0.82 indicating moderate to strong co-localization of intensity distributions between the LAMP1 and FND particles. The Manders' M1 and M2 values indicate significant overlap between the red and green pixels for our samples, except for control sample, as expected. Additional confirmation of co-localization is Li's ICQ, which indicates

moderate co-localization between the LAMP1 stain and FNDs (0.312) samples (0.07). Taken all evidence together, we conclude that the FNDs localize to the lysosome organelles (LAMP1) in the CHO-K1 (**Table 1**).

In conclusion, we demonstrated large scale production of FNDs containing NIR emitters (SiV) suitable for biological labeling. We further show convincing evidence for co-localized uptake of FNDs containing SiV or NV color centers into cells with no apparent toxicity and can be visualized using a standard confocal set-up. FNDs promote cell-induced aggregation of nanoparticles over time that most likely correlates to an autophagy process inside cells. Finally, co-localization study demonstrates that after a prolong incubation the FNDs are located inside late endosomes/lysosome. Our results provide an important stepping stone for the effective use of FNDs multi-color bio-imaging applications, showing that FNDs are a promising biomedical research tool.

FIGURES

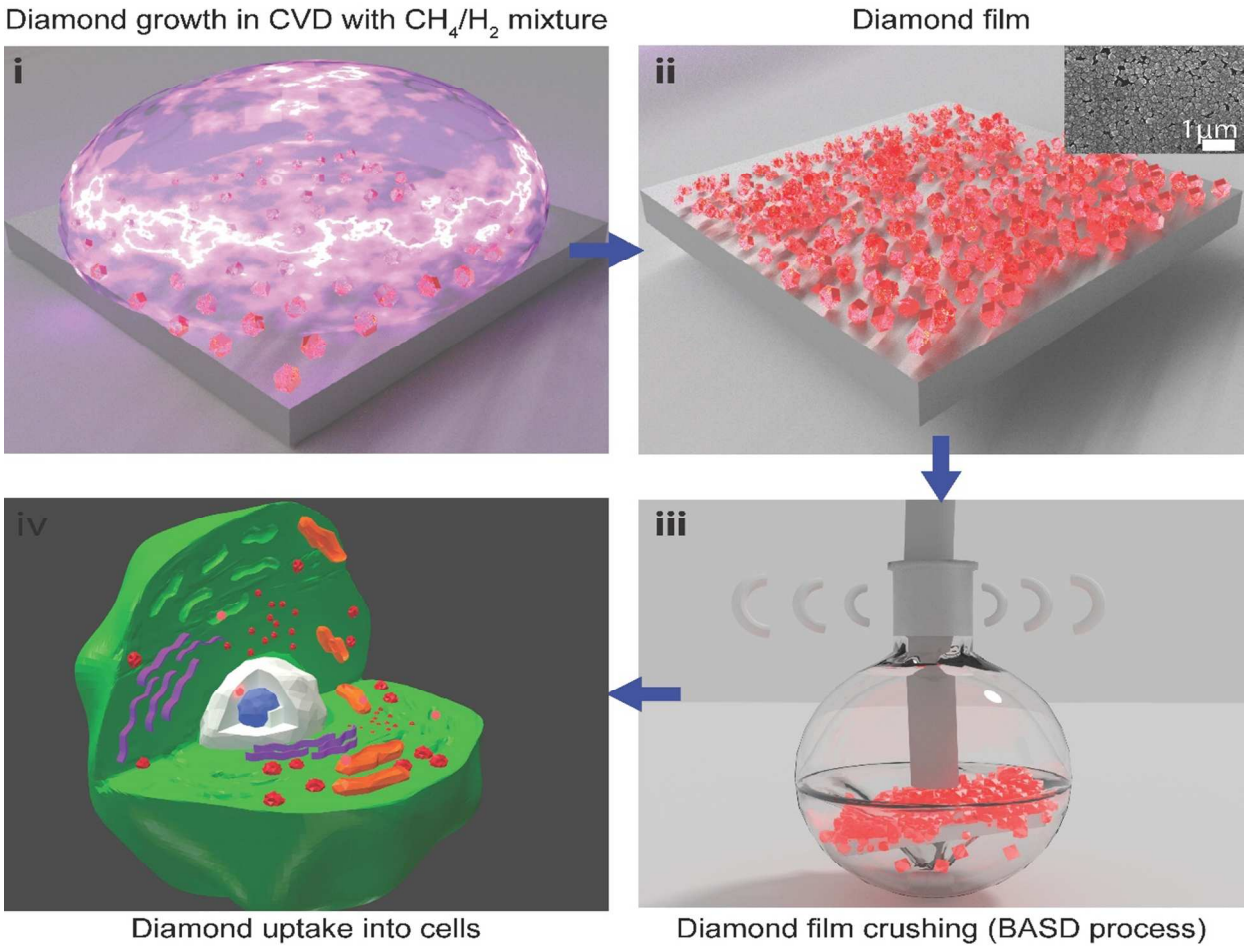

Figure 1. Synthesis of SiV containing FNDs (i). Silicon substrate seeded with detonation nanodiamond (4-5 nm) is subjected to CVD plasma using a standard hydrogen/methane gas mixture to produce highly dense polycrystalline diamond thin film (ii). SEM micrograph (inset) shows diamond thin film of SiV containing FNDs crystals. The CVD diamond film was isolated and was subjected to the BASD process (iii). To remove residual particles and graphite, the diamond solution then underwent strong acid reflux for 24 hours, washed through centrifugation with water to produce SiV FNDs in solution for intercellular bio-imaging (iv).

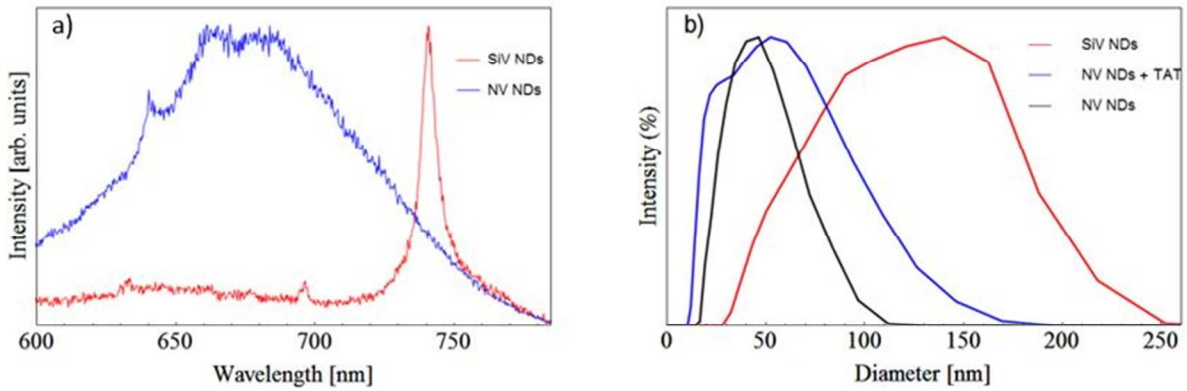

Figure 2. Characterization of different types of FNDs. (a) Normalized, typical room temperature spectra of SiV (red) and NV (blue) color centers under a 532 nm excitation source. Two spectra can be clearly separated based on their optical properties. (b) Particle size distribution by number of SiV (red), NV (black) and NV containing FNDs with TAT (blue) showing sizes <150 nm in diameter.

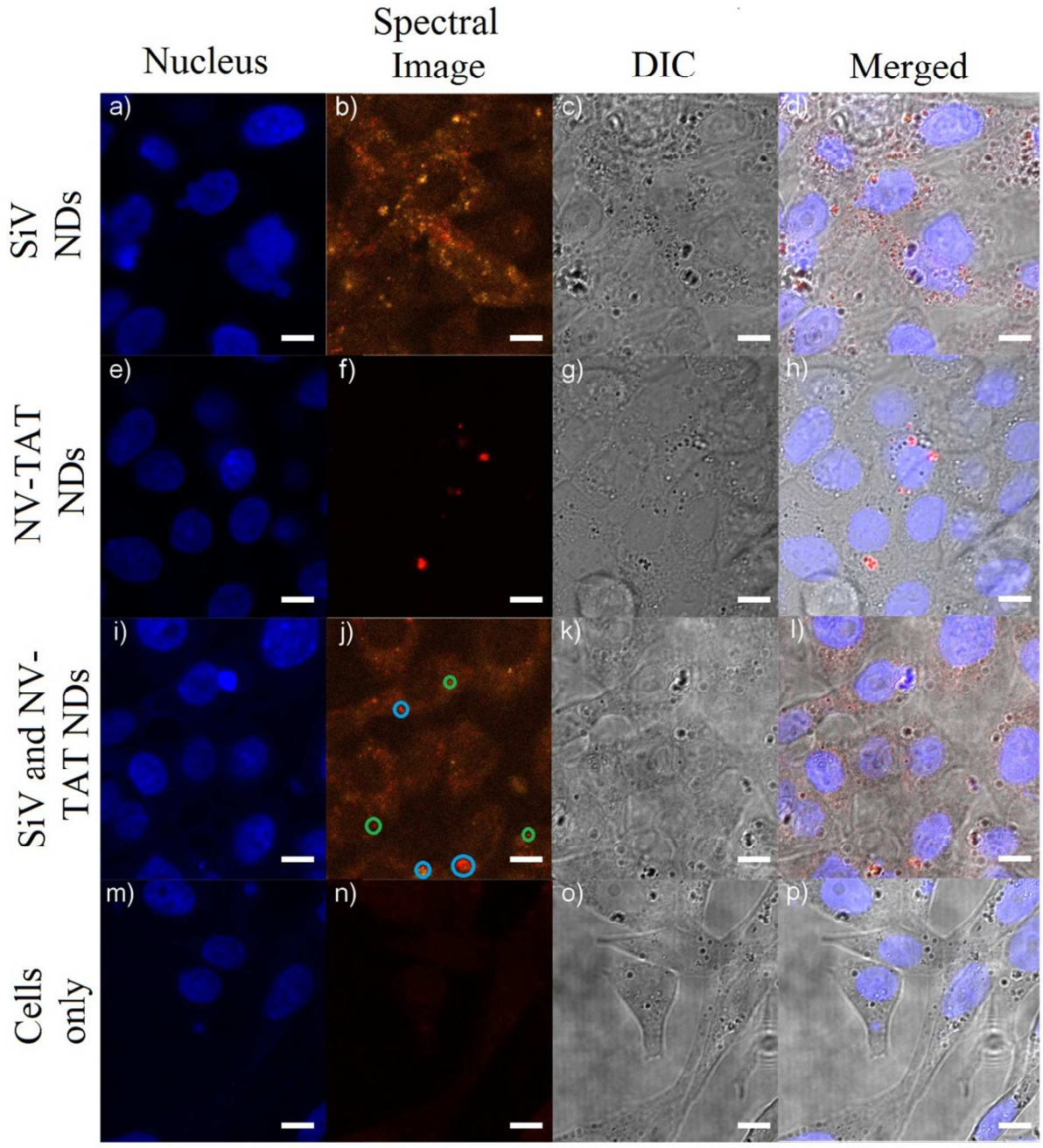

Figure 3. Confocal laser scanning microscopy of fixed CHO-K1 cells. Cells containing FNDs hosting SiV (a-d), NV (e-h), both SiV and NV-TAT (i-l) and control CHO-K1 cells (m-p) were imaged using confocal microscopy. 405 nm excitation (a, e, i, m) shows the NucBlue stained nucleus of the cells. 561 nm excitation collected by a spectrometer (b, f, l, n) shows the bright emission from the various FNDs color centers (localized red spheres). A number of the NV (blue circles) and SiV (green circles) color centers are labelled for clarity. The NV emitters

preferentially accumulate at the periphery of the nucleus, while the SiV emitters are dispersed throughout the cell cytoplasm. A bright field image (c, g, k, o) and merged (d, h, l, p) image shows the cellular membrane and scanned area of interest. The scale bars are 10 μm.

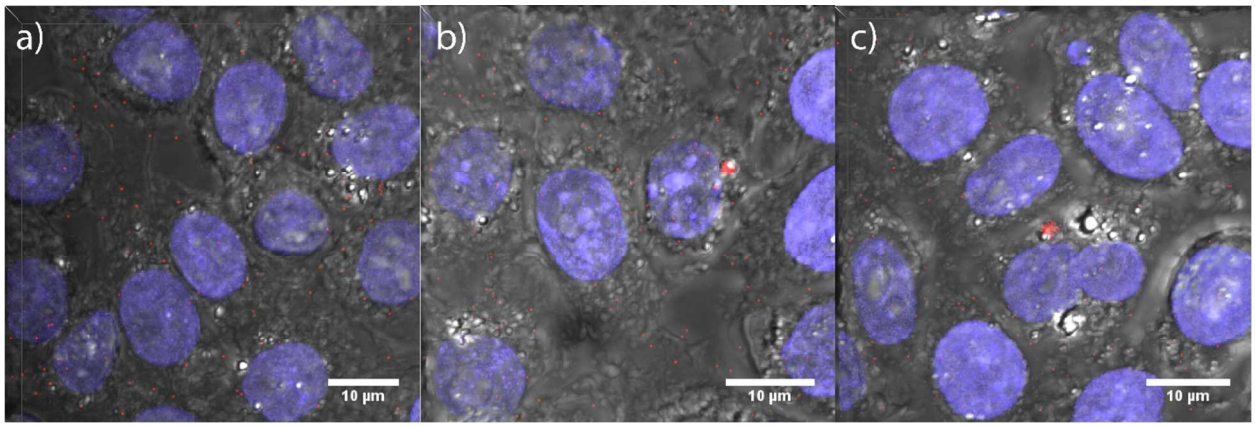

Figure 4. 3D reconstruction of confocal raster scan ofCHO-K1 cells hosting (a) SiV (b) NV (c) both SiV and NV-TAT containing FNDs. 405 nm laser excitation (a, e, i, m) shows the NucBlue stained nucleus of the cells, 561 nm laser excitation was used to reduce cell auto-fluorescence and maximize the collected signal from the FNDs particles. Different angle from the 3D reconstruction of CHO-K1 cells can be seen in Figure S6.

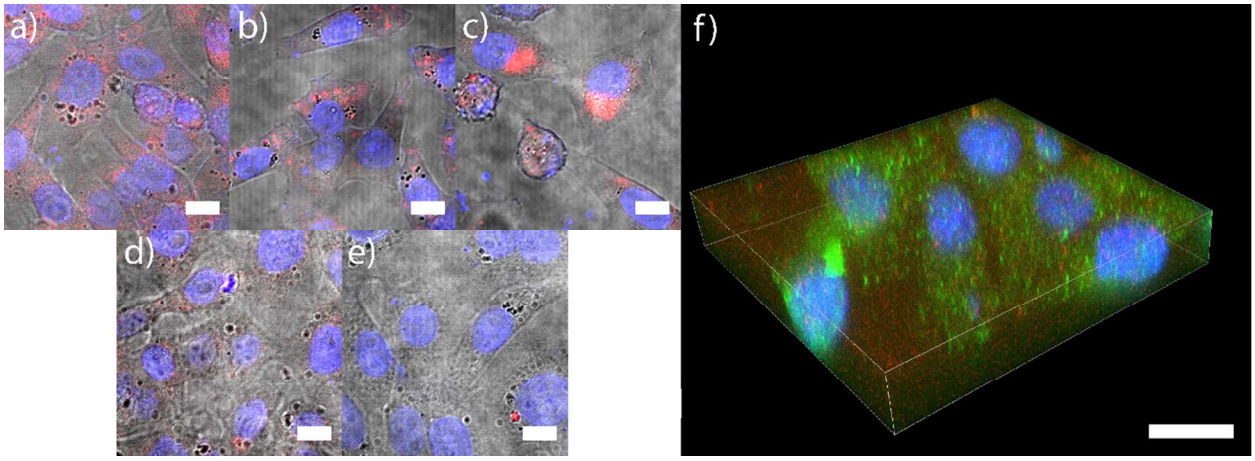

Figure 5. Uptake time study for two types of FNDs (NV-TAT and SiV color centers) together. The cells hosting the FNDs particles were fixed after (a) 5 min, (b) 30 min, (c) 60 min, (d) 180 min and (e) 300 min, they were imaged with a 405 nm and 561 nm laser excitation source. NucBlue stained nucleus of the cells. The FNDs are initially dispersed (a) but over time agglomerate near the cell nucleus (b-e). Scale bar 10 μm. Co-localization imaging of FNDs against primary LAMP1 (f) proteins stained the endosomes or lysosomes. Secondary anti-mouse Alexa Fluor 488 antibodies were used to visualize primary LAMP1 antibodies. Scale bar 20 μm.

TABLES

Table 1. Co-localization test for control and stained cells. The LAMP1 shows co-localization as the Pearson's R value tends towards 1.

Sample	Pearson's R (no Threshold)	Manders' M1/M2	Costes P-Value	Li's ICQ
Cells only (Red vs Green)	0.00	0.01/0.27	0.98	0.112
LAMP1 (Red vs Green)	0.82	1.00/1.00	1.00	0.312

ASSOCIATED CONTENT

Supporting Information. Detailed experimental section; characterization of fabricated diamond films and particles for physical and optical properties; characterization of various FNDs samples for sizes and zeta potential; cell viability assays of FNDs in CHO-K1 and macrophage cells; confocal laser scanning microscopy of FNDs in cell and spectral unmixing; estimation of FNDs type using confocal laser scanning microscopy in fixed CHO-K1 cells; 3D reconstruction of confocal raster scan of CHO-K1 cells hosting SiV and NV-TAT containing FNDs; 3D reconstruction of confocal raster scan of U937 cells induced to macrophages hosting SiV and NV-TAT containing FNDs.

The following files are available free of charge.

AUTHOR INFORMATION

Corresponding Author

*Dr Olga Shimoni

olga.shimoni@uts.edu.au

Funding Sources

I.A., S.V. and O.S. acknowledge the support of Australian Research Council and National Health and Medical Research Council (IH150100028, APP1101258).

ACKNOWLEDGMENT

We would like to acknowledge Michael Johnson and Robert Wooley for their assistance with the confocal microscopy, and Mika Westerhausen for useful discussions.

ABBREVIATIONS

BASD, bead-assisted sonication disintegration; CHO K1, Chinese Hamster Ovarian cell line; CPP, cell penetrating peptide; CVD, chemical vapor deposition; FNDs, fluorescent nanodiamond particles; ICQ, Li's intensity correction quotient ; LAMP1, Lysosomal-associated membrane protein; NIR, near-infrared; NV, nitrogen-vacancy center; SiV, silicon-vacancy center; TAT, trans-activating transcriptional activator ; ZPL, zero phonon line;

REFERENCES

(1) Y. Urano, *Curr. Opin. Chem. Biol.* **2012**, *16*, 602-608.

(2) T.-J. Wu, Y.-K. Tzeng, W.-W. Chang, C.-A. Cheng, Y. Kuo, C.-H. Chien, H.-C. Chang, J. Yu, *Nat. Nanotechnol.* **2013**, *8*, 682-689.

(3) R. S. Kathayat, Y. Cao, P. D. Elvira, P. A. Sandoz, M.-E. Zaballa, M. Z. Springer, L. E. Drake, K. F. Macleod, F. G. van der Goot, B. C. Dickinson, *Nat Comm,* **2018**, 9, 334.

(4) H. C. Davis, P. Ramesh, A. Bhatnagar, A. Lee-Gosselin, J. F. Barry, D. R. Glenn, R. L. Walsworth, M. G. Shapiro, *Nat Comm*, **2018**, 9, 131.

(5) M. Collot, T. K Fam, P. Ashokkumar, O. Faklaris, T. Galli, L. Danglot, A. S. Klymchenko, *J. Am. Chem. Soc.,* **2018**, 0002-7863.

(6) U. Resch-Genger, M. Grabolle, S. Cavaliere-Jaricot, R. Nitschke, T. Nann, *Nat. Methods* **2008**, *5*, 763-775.

(7) J. Geys, A. Nemmar, E. Verbeken, E. Smolders, M. Ratoi, M. F. Hoylaerts, B. Nemery,; P. H. M. Hoet, *Environ. Health Perspect.* **2008**, *116*, 1607-1613.

(8) International Technology Center, http://www.itc-inc.org/ftir_fl.html, **2013.**

(9) J.-C. Arnault, T. Petit, H. Girard, A. Chavanne, C. Gesset, M. Sennourb, M. Chaigneauc, *Phys. Chem. Chem. Phys.* **2011,** 13, 11481-11487.

(10) I. Aharonovich, E. Neu, *Adv. Opt. Mater.* **2014**, *2*, 911-928.

(11) I. Aharonovich, A. D. Greentree, S. Prawer, *Nat. Photonics* **2011**, *5*, 397-405.

(12) W. W.-W. Hsiao, Y. Y. Hui, P.-C. Tsai, H.-C. Chang, *Acc. Chem. Res.* **2016**, *49*, 400-407.

(13) I. P. Chang, K. C. Hwang, J.-A. A. Ho, C.-C. Lin, R. J. R. Hwu, J.-C. Horng, *Langmuir* **2010**, *26*, 3685-3689.

(14) V. N. Mochalin, O. Shenderova, D. Ho, Y. Gogotsi, *Nat. Nanotechnol*. **2012**, *7*, 11-23.

(15) C.-C. Fu, H.-Y. Lee, K. Chen, T.-S. Lim, H.-Y. Wu, P.-K. Lin, P.-K. Wei, P.-H. Tsao, H.-C. Chang, W. Fann, *Proc. Natl. Acad. Sci. U. S. A.* **2007**, *104*, 727-732.

(16) G. Balasubramanian, A. Lazariev, S. R. Arumugam, D. W. Duan, *Curr. Opin. Chem. Bio.l* **2014**, *20*, 69-77.

(17) O. Shimoni, B. Shi, P. A. Adlard, A. I. Bush, *J. Molec. Neurosci*. **2016**, *60*, 405-409.

(18) A. Alhaddad, M. P. Adam, J. Botsoa, G. Dantelle, S. Perruchas, T. Gacoin, C. Mansuy, S. Lavielle, C. Malvy, F. Treussart, J. R Bertrand, *Small* **2011**, *7*, 3087-3095.

(19) J. Li, Y. Zhu, W. Li, X. Zhang, Y. Peng, Q. Huang, *Biomaterials* **2010**, *31*, 8410-8418.

(20) D. A. Simpson, J.-P. Tetienne, J. M. McCoey, K. Ganesan, L. T. Hall, S. Petrou, R. E. Scholten, L. C. L. Hollenberg, *Sci. Rep.* **2016**, *6*, 1-8.

(21) K. Bray, R. Previdi, B.C. Gibson, O. Shimoni, I. Aharonovich, *Nanoscale* **2015**, *7*, 4869-4874.

(22) L. P. McGuinness, Y. Yan, A. Stacey, D.A. Simpson, L.T. Hall, D. Maclaurin, S. Prawer, P. Mulvaney, J. Wrachtrup, F. Caruso, R.E. Scholten, L.C.L. Hollenberg, *Nat. Nanotechnol.* **2011**, *6*, 358-363.

(23) P. Reineck, B.C. Gibson, *Adv. Opt. Mater.* **2016**, *5*, 1-26.

(24) I.I. Vlasov, A.A. Shiryaev, T. Rendler, S. Steinert, S.-Y. Lee, D. Antonov, M. Vörös, F. Jelezko, A.V. Fisenko, L.F. Semjonova, J. Biskupek, U. Kaiser, O.L. Lebedev, I. Sildos, P.R. Hemmer, V.I. Konov, A. Gali, J. Wrachtrup, *Nat. Nanotechnol.* **2014**, *9*, 54-8.

(25) H. Mojarradi, *Dissertation,* **2010.**

(26) E. Neu, C. Arend, E. Gross, F. Guldner, C. Hepp, D. Steinmetz, E. Zscherpel, S. Ghodbane, H. Sternschulte, D. Steinmüller-nethl, Y. Liang, A. Krueger, C. Becher, *Appl. Phys. Lett.* **2011**, *98*, 98-100.

(27) S. Heyer, W. Janssen, S. Turner, Y.-G. Lu, W.S. Yeap, J. Verbeeck, K. Haenen, A. Krueger, *ACS Nano* **2014**, *8*, 5757-5764.

(28) V. N. Mochalin, O. Shenderova, D. Ho, Y. Gogotsi, *Nat. Nano.,* **2012**, 7, 11-23.

(29) S. Fawell, J. Seery, Y. Daikh, C. Moore, L.L. Chen, B. Pepinsky, J. Barsoum, *Proc. Natl. Acad. Sci. U. S. A.* **1994**, *91*, 664-668.

(30) S.A. Moschos, S.W. Jones, M.M. Perry, A.E. Williams, J.S. Erjefalt, J.J. Turner, P.J. Barnes, B.S. Sproat, M.J. Gait, M.A. Lindsay, *Bioconjugate Chem.* **2007**, *18*, 1450-1459.

(31) S. Lim, W.-J. Kim, Y.-H. Kim, S. Lee, J.-H. Koo, J.-A. Lee, H. Yoon, D.-H. Kim, H.-J. Park, H.-M. Kim, H.-G. Lee, J. Yun-Kim, J.-U. Lee, J. Hun-Shin, L. Kyun-Kim, J. Doh, H. Kim, S.-K. Lee A.L.M. Bothwell, M. Suh, J.-M. Choi, *Nature Comms.* **2015**, *6*, 8244.

(32) V.K.A. Sreenivasan, W.A. Razali, K. Zhang, R.R. Pillai, A. Saini, D. Denkova, M. Santiago, H. Brown, J. Thompson, M. Connor, E.M. Goldys, A.V. Zvyagin, *ACS Appl. Mater. Interfaces* **2017**, *9*, 39197-39208.

(33) O. Faklaris, V. Joshi, T. Irinopoulou, P. Tauc, M. Sennour, H. Girard, C. Gesset, J.-C. Arnault, A. Thorel, J.-P. Boudou, P.A. Curmi, F. Treussart, *ACS Nano* **2009**, *3*, 3955-3962.

(34) Y.-A. Huang, C.-W. Kao, K.-K. Liu, H.-S. Huang, M.-H. Chiang, C.-R. Soo, H.-C. Chang, T.-W. Chiu, J.-I. Chao, E. Hwang, *Sci. Rep.* **2014**, *4*, 6919.

(35) Z. Chu, K. Miu, P. Lung, S. Zhang, S. Zhao, H.-C. Chang, *Sci. Rep.* **2015**, *5*, 11661.

(36) N. Prabhakar, M.H. Khan, M. Peurla, H.-C. Chang, P.E. Hänninen, J.M. Rosenholm, *ACS Omega* **2017**, *2*, 2689-2693.

(37) Z. Chu, S. Zhang, B. Zhang, C. Zhang, C.-Y. Fang, I. Rehor, P. Cigler, H.-C. Chang, G. Lin, R. Liu, Q. Li, *Sci. Rep.* 2014, 4, 4495.

(38) M. Liu, Q. Li, L. Liang, J. Li, K. Wang, J. Li, M. Lv, N. Chen, H. Song, J. Lee, J. Shi, L. Wang, R. Lal, C. Fan, *Nature Comms.* **2017**, *8*, 15646.

(39) V.R. Lopes, V. Loitto, J.N. Audinot, N. Bayat, A.C. Gutleb, S. Cristobal, *J. Nanobiotechnol.* **2016**, *14*, 1-13.

(40) D. Huang, H. Zhou, J. Gao, *Sci. Rep.* **2015**, *5*, 14361.

(41) A. Mishra, J. Zheng, X. Tang, P.L. Goering, *Toxicol. Sci.* **2016**, *150*, 473-487.

(42) E. Panzarini, L. Dini, *Molec. Pharma*. **2014**, *11*, 2527-2538.

Table of contents

We report on the first demonstration of FNDs containing either silicon or nitrogen vacancy color centers for multi-color bio-imaging.

.

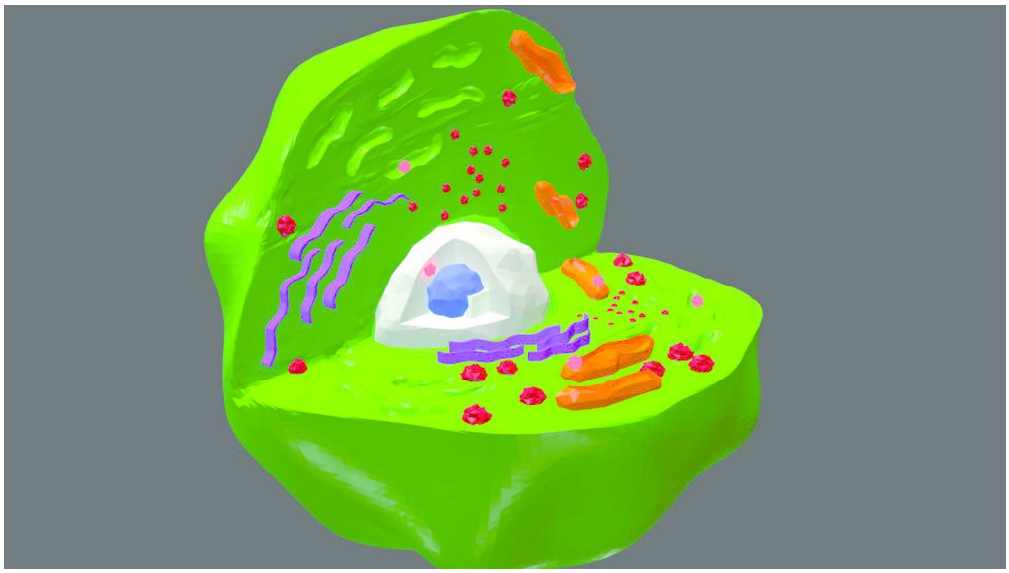

677x381mm (72 x 72 DPI)